European Society of Computational Methods in Sciences and Engineering (ESCMSE)

Journal of Numerical Analysis, Industrial and Applied Mathematics (JNAIAM)
vol. 3, no. 3-4, 2008, pp. 181-191
ISSN 1790–8140

Numerical Aspects of the Coefficient Computation for LMMs[1]

L. Aceto[2]

Dipartimento di Matematica Applicata,
Università di Pisa,
Via Buonarroti 1/c,
56127 Pisa, Italy

A. Sestini[3]

Dipartimento di Matematica,
Università di Firenze,
Viale Morgagni 67a,
50134 Firenze, Italy

Received 25 January, 2008; accepted in revised form 26 August, 2008

Abstract: The numerical solution of Boundary Value Problems usually requires the use of an adaptive mesh selection strategy. For this reason, when a Linear Multistep Method is considered, a dynamic computation of its coefficients is necessary. This leads to solve linear systems which can be expressed in different forms, depending on the polynomial basis used to impose the order conditions. In this paper, we compare the accuracy of the numerically computed coefficients for three different formulations. For all the considered cases Vandermonde systems on general abscissae are involved and they are always solved by the Björk-Pereyra algorithm [3]. An adaptation of the forward error analysis given in [8, 9] is proposed whose significance is confirmed by the numerical results.

Keywords: Linear Multistep Methods, Boundary Value Methods, Conditioning, Vandermonde matrix, Bernstein polynomials, Björk-Pereyra algorithm

Mathematics Subject Classification: 65L06, 65L10, 65F95

1 Introduction

Dealing with a Boundary Value Problem (BVP)

$$\begin{cases} \mathbf{y}'(x) = \mathbf{f}(x, \mathbf{y}(x)), & a < x < b, \\ \mathbf{g}(\mathbf{y}(a), \mathbf{y}(b)) = \mathbf{0}, \end{cases} \tag{1}$$

[1]Published electronically October 15, 2008
[2]Corresponding author. E-mail: l.aceto@dma.unipi.it
[3]E-mail: sestini@math.unifi.it

with $\mathbf{y} \in \mathbb{R}^d, d \geq 1$, $\mathbf{f}$ and $\mathbf{g}$ sufficiently smooth functions, a possible numerical approach is based on a suitable use of Linear Multistep Methods (LMMs), that is on their formulation in the general context of Boundary Value Methods (BVMs) [4]. In order to reduce the computational cost when difficult problems are considered, variable–step meshes have to be used and they are usually adaptively computed by the codes (see, for example, [10]). This implies the necessity of a dynamical updating of the coefficients characterizing the numerical scheme because each of them depends on a finite number of ratios between consecutive stepsizes. Obviously, the behavior of the numerical solution can also be influenced by the accuracy of the numerical computation of such coefficients. This is the reason why we were interested in this topic.
The determination of the LMMs' coefficients usually requires to solve Vandermonde-like systems which can be formulated using different polynomial bases. In particular, in this paper we have considered for the Extended Trapezoidal Rules (ETRs) the monomial basis combined with two different linear mappings and the Bernstein basis, which in the following will be referred to respectively by the labels MON1, MON2 and BERN. Each of these choices leads to the solution of Vandermonde systems with a specific set of strictly increasing abscissae which are nonnegative only for MON1 and BERN. In all the considered cases the algorithm selected for their solution is the Björk-Pereyra algorithm [3] which has a quadratical computational cost with respect to the system size. The numerical experiments here reported together with analogous ones performed for other classes of LMMs (e.g. the Generalized BDFs considered in [1]) confirm that significant different accuracy can be obtained using the previously mentioned formulations. In particular, BERN and MON2 always are capable to produce highly accurate coefficients even if for some classes of methods BERN requires particular care to compute the right–hand side of the considered linear systems. On the other hand, MON1 always gives worst accuracy. The behavior of MON1 and BERN can be a priori explained considering the forward error analysis given in [8, 9] which applies since the involved abscissae in the Vandermonde matrices are nonnegative. An analogous explanation of the good results produced by MON2 can be obtained by using an adaptation of such analysis to the case of general sets of strictly increasing abscissae.

The paper is organized as follows. In Section 2 the order conditions on a not necessarily uniform mesh are reported when a LMM is used in the general setting of BVMs. In addition, they are particularized to the case of the ETRs. In Section 3 the order conditions for the ETRs are suitably formulated in three different forms, all requiring the solution of Vandermonde systems. For solving such systems the Björk-Pereyra algorithm has been always used. A sketch of it, together with the related stability analysis is reported in Section 4. Finally, some numerical results are given in Section 5 where three mesh distributions are considered for the experiments.

2 Order conditions

Let $\pi = \{a = x_0 < x_1 < \ldots < x_N = b\}$ denote any assigned mesh in the integration interval $[a, b]$ and let $h_i = x_i - x_{i-1}$. Then the associated numerical solution $\{\mathbf{y}_i, i = 0, \ldots, N\}$ of (1) defined by

a k–step LMM used in the general setting of BVMs [4] has to satisfy the following equations,

$$\begin{aligned}
\sum_{j=-i}^{k-i} \alpha_{i+j}^{(i)}\, \mathbf{y}_{i+j} &= h_i \sum_{j=-i}^{k-i} \beta_{i+j}^{(i)}\, \mathbf{f}_{i+j}, \quad i = 1, \ldots, \nu-1,\\
\sum_{j=-\nu}^{k-\nu} \alpha_{j+\nu}^{(i)}\, \mathbf{y}_{i+j} &= h_i \sum_{j=-\nu}^{k-\nu} \beta_{j+\nu}^{(i)}\, \mathbf{f}_{i+j}, \quad i = \nu, \ldots, N-k+\nu,\\
\sum_{j=N-i-k}^{N-i} \alpha_{i+j-N+k}^{(i)}\, \mathbf{y}_{i+j} &= h_i \sum_{j=N-i-k}^{N-i} \beta_{i+j-N+k}^{(i)}\, \mathbf{f}_{i+j}, \quad i = N-k+\nu+1, \ldots, N,\\
\mathbf{g}(\mathbf{y}(a), \mathbf{y}(b)) &= \mathbf{0},
\end{aligned}$$

where $\mathbf{f}_\ell = \mathbf{f}(x_\ell, \mathbf{y}_\ell), \ell = 0, \ldots, N$, the integer ν, $1 \le \nu \le k$, has to be appropriately chosen for stability reasons [4] (it is equal to k if the LMM can be used as a classical Initial Value Method) and the coefficients $\{\alpha_r^{(i)}\}$ and $\{\beta_r^{(i)}\}$, $r = 0, \ldots, k$, $i = 1, \ldots, N$, characterize the methods on the assigned mesh. More specifically, when $i = \nu, \ldots, N-k+\nu$, they characterize the *main* methods and, otherwise, the *additional* left and right methods.

In this paper we are interested in studying the accuracy of the numerical computation of the coefficients $\{\alpha_r^{(i)}\}$ and $\{\beta_r^{(i)}\}$, $r = 0, \ldots, k$, $i = 1, \ldots, N$. For brevity, in the sequel we only consider the main methods because analogous considerations can be made for the additional ones.

In [4] some classical LMMs are revisited and some new generalizations are also introduced. For most of them one of $\boldsymbol{\alpha}^{(i)} = (\alpha_0^{(i)}, \ldots, \alpha_k^{(i)})^T$ or $\boldsymbol{\beta}^{(i)} = (\beta_0^{(i)}, \ldots, \beta_k^{(i)})^T$ is a priori assigned and the other is computed using the order conditions (see below). A significant exception is represented by the class of BS methods, introduced and analyzed in [11, 12, 13], of order $k+1$, whose coefficients are computed by a different strategy. The numerical solution produced by such methods admits a continuous extension given by a collocation spline sharing with it the convergence order.

Usually the monomial basis is used for imposing the order conditions. This leads to write the p–order conditions for the main methods, with $p \le 2k$, in matrix form as follows

$$V_p(x_{i-\nu}, \ldots, x_{i+k-\nu})\, \boldsymbol{\alpha}^{(i)} \;=\; h_i\, H_p\, V_p(x_{i-\nu}, \ldots, x_{i+k-\nu})\, \boldsymbol{\beta}^{(i)}, \quad i = \nu, \ldots, N-k+\nu, \tag{2}$$

where the Vandermonde matrix is given by

$$V_p(x_{i-\nu}, \ldots, x_{i+k-\nu}) \;=\; \begin{pmatrix} 1 & 1 & \cdots & 1 \\ x_{i-\nu} & x_{i+1-\nu} & \cdots & x_{i+k-\nu} \\ \vdots & \vdots & \vdots & \vdots \\ x_{i-\nu}^p & x_{i+1-\nu}^p & \cdots & x_{i+k-\nu}^p \end{pmatrix}_{(p+1)\times(k+1)}$$

and $H_p \in \mathbb{R}^{(p+1)\times(p+1)}$ is the matrix whose entries are $(H_p)_{i,j} = j\delta_{i,j+1}$, $i, j = 0, 1, \ldots, p$, with $\delta_{r,s}$ denoting the Kronecker delta, as usual.

In the following we focus on a special class of LMMs which is called ETRs (Extended Trapezoidal Rules) [4]. Such methods generalize to each odd number k of steps the classical trapezoidal rule. ETRs are here considered because they are suited for solving BVPs (see, for example, their implementation in the code TOM, [10]). In this case, for each fixed $k = 2\nu - 1$, $\nu \ge 1$, the entries of the coefficient vector $\boldsymbol{\alpha}^{(i)}$ are a priori assigned all equal to 0, except for $\alpha_{\nu-1}^{(i)} = -1$ and $\alpha_\nu^{(i)} = 1$. The entries of the coefficient vector $\boldsymbol{\beta}^{(i)}$ are then uniquely determined by imposing the conditions (2) with $p = k+1$. In fact, in this case the first equation in (2) is trivially satisfied for any $\boldsymbol{\beta}^{(i)}$ and the remaining $k+1$ equations can be more conveniently stated as follows:

$$V_k(x_{i-\nu}, \ldots, x_{i+k-\nu})\, \boldsymbol{\beta}^{(i)} \;=\; h_i^{-1}\, \mathbf{v}^{(i)}, \quad i = \nu, \ldots, N-k+\nu, \tag{3}$$

where $\mathbf{v}^{(i)} = (x_i - x_{i-1}, (x_i^2 - x_{i-1}^2)/2, \ldots, (x_i^{k+1} - x_{i-1}^{k+1})/(k+1))^T$.

3 Reformulations of the order conditions

The formulation of the order conditions for the k-step ETR method given in (3) depends on the amplitude of the integration interval. We can overcome this fact by multiplying on the left both the terms in (3) by a suitable matrix. In particular, for this aim two analogous matrices will be considered, say $P_1^{(i)}$ and $P_2^{(i)}$, defined as follows:

$$P_1^{(i)} = \left(P(x_{i-\nu})\, D(\hat{h}_i)\right)^{-1}, \qquad P_2^{(i)} = \left(P(x_i)\, D(h_i)\right)^{-1}, \tag{4}$$

where $D(\gamma) = \text{diag}\ (1, \gamma, \ldots, \gamma^k)$, for each $\gamma \in \mathbb{R}\backslash\{0\}$, $\hat{h}_i = \sum_{j=1}^{k} h_{i-\nu+j}$ and $P(y)$ is the generalized Pascal matrix having the following entries:

$$[P(y)]_{rs} = \begin{cases} \binom{r}{s} y^{r-s} & \text{if } r \geq s, \\ 0 & \text{otherwise,} \end{cases} \qquad r, s = 0, 1, \ldots, k,$$

which transforms the vector

$$\mathbf{w}(x) = (1, x, x^2, \ldots, x^k)^T \tag{5}$$

into the vector

$$P(y)\, \mathbf{w}(x) = \left(1, (x+y), (x+y)^2, \ldots, (x+y)^k\right)^T \tag{6}$$

as shown, for example, in [2].
By using these matrices, (3) can be replaced by one of the two following systems:

$$V_k(\xi_0^{(i,j)}, \ldots, \xi_k^{(i,j)})\, \boldsymbol{\beta}^{(i)} = \mathbf{t}^{(i,j)}, \qquad i = \nu, \ldots, N-k+\nu, \quad j = 1, 2, \tag{7}$$

where $\mathbf{t}^{(i,j)} = h_i^{-1}\, P_j^{(i)}\, \mathbf{v}^{(i)}$ and the sets of abscissae are

$$\left\{\xi_0^{(i,1)}, \ldots, \xi_k^{(i,1)}\right\} = \left\{0, \frac{h_{i-\nu+1}}{\hat{h}_i}, \frac{h_{i-\nu+1} + h_{i-\nu+2}}{\hat{h}_i}, \ldots, 1\right\}, \tag{8}$$

$$\left\{\xi_0^{(i,2)}, \ldots, \xi_k^{(i,2)}\right\} = \left\{-\frac{\sum_{r=1}^{\nu} h_{i-\nu+r}}{h_i}, \ldots, -\frac{h_{i-1} + h_i}{h_i}, -1, 0, \frac{h_{i+1}}{h_i}, \ldots, \frac{\sum_{r=1}^{k-\nu} h_{i+r}}{h_i}\right\}. \tag{9}$$

As proved in the Appendix, when $j = 2$ the entries of the right hand side in (7) have the following very simple form:

$$\left[\mathbf{t}^{(i,2)}\right]_r = \left[h_i^{-1}\, P_2^{(i)}\, \mathbf{v}^{(i)}\right]_r = \frac{(-1)^r}{r+1}, \qquad r = 0, 1, \ldots, k. \tag{10}$$

In the sequel we relate to the formulations in (7) by using the labels MON1 when $j = 1$ and MON2 when $j = 2$, respectively. In addition, a third formulation is also considered. In this case both the terms in (3) are multiplied on the left by the matrix $P_3^{(i)}$ defined as follows:

$$P_3^{(i)} = T\, P_1^{(i)},$$

where T is the upper triangular matrix given by

$$[T]_{rs} = \begin{cases} \binom{k}{r}\binom{k-r}{k-s}(-1)^{s-r} & \text{if } r \le s, \\ 0 & \text{otherwise,} \end{cases} \qquad r,s = 0,1,\ldots,k.$$

The matrix T realizes the change of basis from the monomials to the Bernstein polynomials and it has been here considered since it is well-known in the literature that the Bernstein basis has good stability features [7]. By using this matrix, the system (3) becomes

$$B_k(\xi_0^{(i,1)},\ldots,\xi_k^{(i,1)})\,\boldsymbol{\beta}^{(i)} = \mathbf{t}^{(i,3)}, \qquad i = \nu,\ldots,N-k+\nu, \tag{11}$$

where the entries of the coefficient matrix $B_k(\xi_0^{(i,1)},\ldots,\xi_k^{(i,1)}) = P_3^{(i)}\,V_k(x_{i-\nu},\ldots,x_{i+k-\nu})$ are the Bernstein polynomials of degree k (see, for example, [6]) evaluated at the abscissae $\left\{\xi_j^{(i,1)}\right\}$, that is

$$\left[B_k(\xi_0^{(i,1)},\ldots,\xi_k^{(i,1)})\right]_{rs} = \binom{k}{r}\left(\xi_s^{(i,1)}\right)^r(1-\xi_s^{(i,1)})^{k-r}, \qquad r,s = 0,1,\ldots,k, \tag{12}$$

and $\mathbf{t}^{(i,3)} = h_i^{-1}\,P_3^{(i)}\,\mathbf{v}^{(i)}$. For brevity, in the following we omit the dependency on the abscissae.

The system in (11) can be solved by using the standard Gauss elimination approach without the need of pivoting because its coefficient matrix is totally positive, (see, for example, [5]). On the other hand, it is also possible to reduce it, after some further algebraic manipulations, to a Vandermonde system. In fact, considering (8) and (12), it can be easily checked that the first and last column of B_k are, respectively, equal to $\mathbf{e}_1$ and $\mathbf{e}_{k+1}$, i.e., to the first and last column of the identity matrix of size $k+1$. Then, denoting by $\tilde{B}_k$ the $(k-1)\times(k-1)$ submatrix of B_k obtained selecting its inner rows and columns, (11) can be replaced by

$$\tilde{B}_k\,\tilde{\boldsymbol{\beta}}^{(i)} = \tilde{\mathbf{t}}^{(i,3)}, \tag{13}$$

where $\tilde{\boldsymbol{\beta}}^{(i)} = (\beta_1^{(i)},\cdots,\beta_{k-1}^{(i)})^T$ and $\tilde{\mathbf{t}}^{(i,3)} \in \mathbb{R}^{k-1}$ is obtained from $\mathbf{t}^{(i,3)}$ removing its first and last entries. After having solved (13), the other two coefficients $\beta_r^{(i)}, r = 0,k$, are obtained by,

$$\begin{aligned} \beta_0^{(i)} &= \mathbf{e}_1^T \left(\mathbf{t}^{(i,3)} - B_k\left(0,\beta_1^{(i)},\ldots,\beta_{k-1}^{(i)},0\right)^T\right), \\ \beta_k^{(i)} &= \mathbf{e}_{k+1}^T \left(\mathbf{t}^{(i,3)} - B_k\left(0,\beta_1^{(i)},\ldots,\beta_{k-1}^{(i)},0\right)^T\right). \end{aligned} \tag{14}$$

Now, taking again into account (12), it can be easily obtained that

$$\tilde{B}_k = D_k\,V_{k-2}(\xi_1^{(i,3)},\ldots,\xi_{k-1}^{(i,3)})\,\hat{D}_i,$$

where D_k and $\hat{D}_i$ are the diagonal matrices defined as

$$D_k = \operatorname{diag}\left(\binom{k}{1},\ldots,\binom{k}{k-1}\right), \quad \hat{D}_i = \operatorname{diag}\left(\xi_1^{(i,1)}(1-\xi_1^{(i,1)})^{k-1},\ldots,\xi_{k-1}^{(i,1)}(1-\xi_{k-1}^{(i,1)})^{k-1}\right),$$

respectively, and

$$\left\{\xi_1^{(i,3)},\ldots,\xi_{k-1}^{(i,3)}\right\} = \left\{\frac{\xi_1^{(i,1)}}{1-\xi_1^{(i,1)}},\ldots,\frac{\xi_{k-1}^{(i,1)}}{1-\xi_{k-1}^{(i,1)}}\right\}. \tag{15}$$

Thus, instead of solving (11) we can solve the following reduced Vandermonde system

$$V_{k-2}(\xi_1^{(i,3)},\ldots,\xi_{k-1}^{(i,3)})\,\left(\hat{D}_i\tilde{\boldsymbol{\beta}}^{(i)}\right) = (D_k)^{-1}\,\tilde{\mathbf{t}}^{(i,3)} \tag{16}$$

and then use (14) to get the full solution of (11). In the sequel we refer to this formulation by the label BERN.

For the numerical solution of the three systems, the two in (7) and that in (16), we have used the Björk–Pereyra algorithm [3] which is specific for solving Vandermonde systems and it is efficient from the point of view of the computational cost. In order to discuss simultaneously the three systems, in the next section such algorithm is briefly introduced for a general Vandermonde system of size $(n+1)$.

4 The Björk-Pereyra algorithm and its stability analysis

We denote by

$$V\,\mathbf{x} = \mathbf{b} \tag{17}$$

a Vandermonde system of size $(n+1)$ with $V = V(\xi_0,\ldots,\xi_n)$, $\xi_0 < \ldots < \xi_n$. It can be solved by using the Björk-Pereyra algorithm [3] whose matrix formulation is here reported. Considering that $V^{-1} = L_0^T\cdots L_{n-1}^T U_{n-1}^T\cdots U_0^T$ with

$$L_i = \begin{pmatrix} I_i & O \\ O & \hat{L}_i \end{pmatrix}, \qquad U_i = \begin{pmatrix} I_i & O \\ O & \hat{U}_i \end{pmatrix}, \qquad i = 0,1,\ldots,n-1,$$

being $I_i \in \mathbb{R}^{i\times i}$ the identity matrix,

$$\hat{L}_i \;=\; \mathrm{diag}\left(1,(\xi_{i+1}-\xi_0)^{-1},\ldots,(\xi_n-\xi_{n-i-1})^{-1}\right)\begin{pmatrix} 1 & 0 & \ldots & \ldots & 0 \\ -1 & \ddots & \ddots & \ddots & \vdots \\ 0 & \ddots & \ddots & \ddots & \vdots \\ \vdots & \ddots & \ddots & \ddots & 0 \\ 0 & \ldots & 0 & -1 & 1 \end{pmatrix},$$

and

$$\hat{U}_i \;=\; \begin{pmatrix} 1 & -\xi_i & 0 & \ldots & 0 \\ 0 & \ddots & \ddots & \ddots & \vdots \\ \vdots & \ddots & \ddots & \ddots & 0 \\ \vdots & \ddots & \ddots & \ddots & -\xi_i \\ 0 & \ldots & \ldots & 0 & 1 \end{pmatrix},$$

then the algorithm has the following two main steps:

$$\begin{aligned} \text{STEP I} \;&:\; \mathbf{d} = U_{n-1}^T\cdots U_0^T\,\mathbf{b} \\ \text{STEP II} \;&:\; \mathbf{x} = L_0^T\cdots L_{n-1}^T\,\mathbf{d}. \end{aligned}$$

From the above expression of the matrices L_i and U_i it can be easily obtained that its asymptotic computational cost is $O(n^2)$; we refer to [3] for further details.

Concerning the stability features of this algorithm, an interesting analysis is reported by Higham in [9]. We use such analysis to compare from the stability point of view the different formulations of the order conditions for ETRs introduced in Section 3.

The following theorem is the analogous for the system (17) of the Theorem 3.1 proved in [9] for the dual system:

Theorem 1 *Let the Björk-Pereyra algorithm be applied in floating point arithmetic to floating point data* $\{\xi_i, b_i\}_{i=0}^n$ *. Provided that no overflows are encountered the algorithm runs to completion, and the computed solution* $\hat{\mathbf{x}}$ *satisfies*

$$|\hat{\mathbf{x}} - \mathbf{x}| \leq c(n,u)\ \left|L_0^T\right| \cdots \left|L_{n-1}^T\right|\ \left|U_{n-1}^T\right| \cdots \left|U_0^T\right|\ |\mathbf{b}|\,,$$

where u *denotes the machine precision and* $c(n,u) = 8\,n\,u + O(u^2)$.

Consequently,

$$err = \frac{\|\hat{\mathbf{x}} - \mathbf{x}\|_\infty}{\|\mathbf{x}\|_\infty} \leq c(n,u)\ \frac{\left\|\ \left|L_0^T\right| \cdots \left|L_{n-1}^T\right|\ \left|U_{n-1}^T\right| \cdots \left|U_0^T\right|\ |\mathbf{b}|\ \right\|_\infty}{\|V^{-1}\,\mathbf{b}\|_\infty}, \tag{18}$$

with $\|\cdot\|_\infty$ denoting the infinity vector norm. We observe that if

$$\xi_0 < \ldots < \xi_{m-1} < 0 \leq \xi_m < \ldots < \xi_n, \qquad 0 \leq m \leq n,$$

then, $U_i \geq 0$ for $i = 0, \ldots, m-1$, and, in addition, the matrices $U_m, \ldots, U_{n-1}$ have alternating sign pattern and similarly for the matrices $L_i, i = 0, 1, \ldots, n-1$. Therefore,

$$\begin{aligned} \left|L_0^T\right| \cdots \left|L_{n-1}^T\right|\ \left|U_{n-1}^T\right| \cdots \left|U_m^T\right|\ \left|U_{m-1}^T\right| \cdots \left|U_0^T\right| &= \left|L_0^T \cdots L_{n-1}^T\, U_{n-1}^T \cdots U_m^T\right|\ U_{m-1}^T \cdots U_0^T \\ &= \left|V^{-1}\,S^{-T}\right|\ S^T, \end{aligned}$$

where we have posed $S^T = U_{m-1}^T \cdots U_0^T$. As a consequence, relation (18) can be written as follows:

$$err \leq c(n,u)\,\omega, \tag{19}$$

with

$$\omega = \frac{\left\|\ \left|V^{-1}\,S^{-T}\right|\ S^T\ |\mathbf{b}|\ \right\|_\infty}{\|V^{-1}\,\mathbf{b}\|_\infty}. \tag{20}$$

Obviously, when all the abscissae are nonnegative, i.e., $m = 0$, the matrix S coincides with the identity matrix and ω reduces to

$$w = \frac{\left\|\ \left|V^{-1}\right|\ |\mathbf{b}|\ \right\|_\infty}{\|V^{-1}\,\mathbf{b}\|_\infty}. \tag{21}$$

In particular, if the right–hand side $\mathbf{b}$ of (17) is any vector of the canonical basis it is $w = 1$. This is also true if its entries have alternate sign and the abscissae of the Vandermonde system are positive (in fact in this case V^{-1} has a chessboard structure).

Proposition 1 *The ratio* w *defined in (21) satisfies the following inequalities*

$$1 \leq w \leq \mu_\infty(V),$$

where $\mu_\infty(V) = \|V\|_\infty\,\|V^{-1}\|_\infty$ *denotes the condition number of the Vandermonde matrix in the infinity norm.*

Proof : Since $\left|V^{-1}\,\mathbf{b}\right| \leq \left|V^{-1}\right|\,|\mathbf{b}|$, one has that

$$\left\|V^{-1}\,\mathbf{b}\right\|_\infty \leq \left\|\,\left|V^{-1}\right|\,|\mathbf{b}|\,\right\|_\infty,$$

which implies $w \geq 1$. Moreover,

$$\left\|\,\left|V^{-1}\right|\,|\mathbf{b}|\,\right\|_\infty = \left\|\,\left|V^{-1}\right|\,\left|V\,V^{-1}\,\mathbf{b}\right|\,\right\|_\infty \leq \mu_\infty(V)\,\left\|\,V^{-1}\,\mathbf{b}\right\|_\infty$$

which completes the thesis. ∎

Concerning the computation of the coefficients for the ETRs by using the Björk-Pereyra algorithm for solving the three considered Vandermonde systems, we remark that the related abscissae (see (8), (9) and (15)) are ordered as follows:

- MON1: $0 \equiv \xi_0^{(i,1)} < \xi_1^{(i,1)} < \cdots < \xi_k^{(i,1)} \equiv 1$;
- MON2: $\xi_0^{(i,2)} < \cdots < \xi_{\nu-1}^{(i,2)} \equiv -1 < 0 \equiv \xi_\nu^{(i,2)} < \cdots < \xi_k^{(i,2)}$;
- BERN: $0 < \xi_1^{(i,3)} < \xi_2^{(i,3)} < \cdots < \xi_{k-1}^{(i,3)}$.

Thus, for all the three formulations we will use (19) to get an a priori estimate for the relative error. (Observe that $\omega = w$ when MON1 and BERN are considered.)

5 Numerical results

The performances of the Björk-Pereyra algorithm for the dynamic computation of the coefficients of the ETRs are tested by solving the linear systems in (7) and in (16) on three different mesh distributions, denoted in the following by UNIF, LGL and GEOM. The first distribution is uniform. In the second case the mesh of size $n+1$ in the interval $[-1\,,\,1]$ is given by the zeros of the polynomial

$$\mathcal{P}_{n+1}(x) = (1-x^2)\,\mathcal{L}'_n(x),$$

with $\mathcal{L}_n(x)$ denoting the Legendre polynomial of degree n. Finally, in the third case the mesh of size $n+1$ is obtained by introducing on a coarser uniform mesh a suitable number of auxiliary nodes with a geometric progression distribution near the extremes of the interval (see [4] for the details). In all the reported experiments the number of steps k is odd and it ranges between 3 and 11 for UNIF and LGL and between 5 and 11 for GEOM.

Figures 1–3 are made by three pictures where the reported results are represented in logarithmic scale and they relate to all the three considered formulations MON1, MON2 and BERN. In particular, from the left, the first and the second pictures show the behaviour of the condition number $\mu_\infty(V)$ of the Vandermonde matrices and that of the parameter ω, respectively. In the last one the relative error *err* versus the step number k is drawn. Looking at the results, we can deduce that the parameter ω gives a more significant bound on the relative error *err* than the condition number. In addition we can also observe that MON2 and BERN are always better than MON1 and that they are almost equivalent.

We remark that in all these figures the right–hand sides of the systems labeled as MON1 and BERN are accurately computed by using symbolic computation (this is not the case for MON2 because its right–hand side has a simple analytic expression, see (10)). In fact, as shown in Figure 4 for the particular case of the uniform distribution, a non accurate computation of this term leads to a deterioration of the dynamical computation of the ETRs' coefficients.

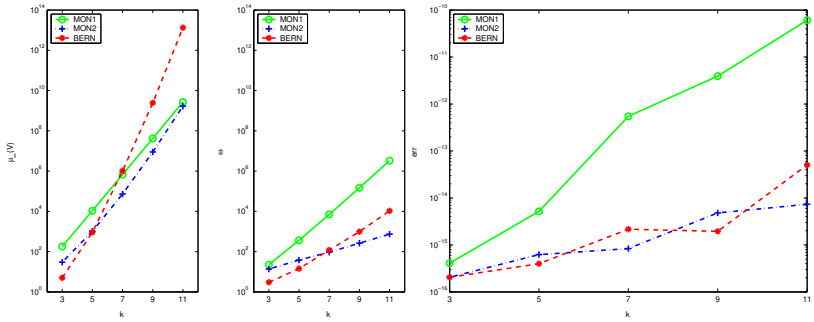

Figure 1: The k–step ETR on a uniform mesh. From left to right: the condition number, the new parameter given in (20) and the relative error bounded in (19) with an accurate computation of the right–hand side.

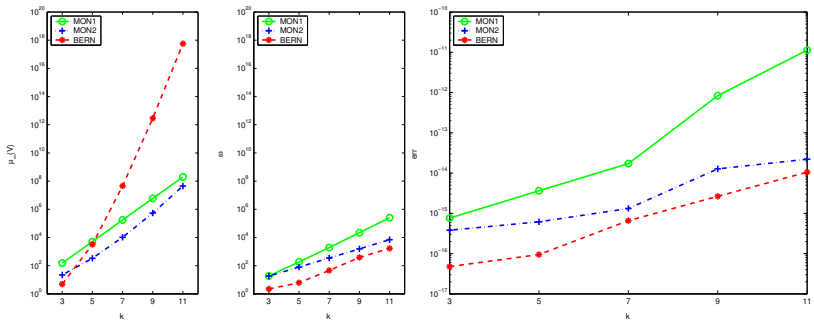

Figure 2: The k–step ETR on the LGL mesh. From left to right: the condition number, the new parameter given in (20) and the relative error bounded in (19) with an accurate computation of the right–hand side.

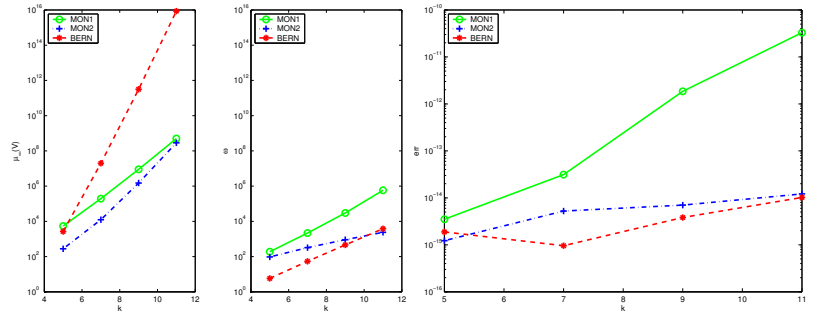

Figure 3: The k–step ETR on the GEOM mesh. From left to right: the condition number, the new parameter given in (20) and the relative error bounded in (19) with an accurate computation of the right–hand side.

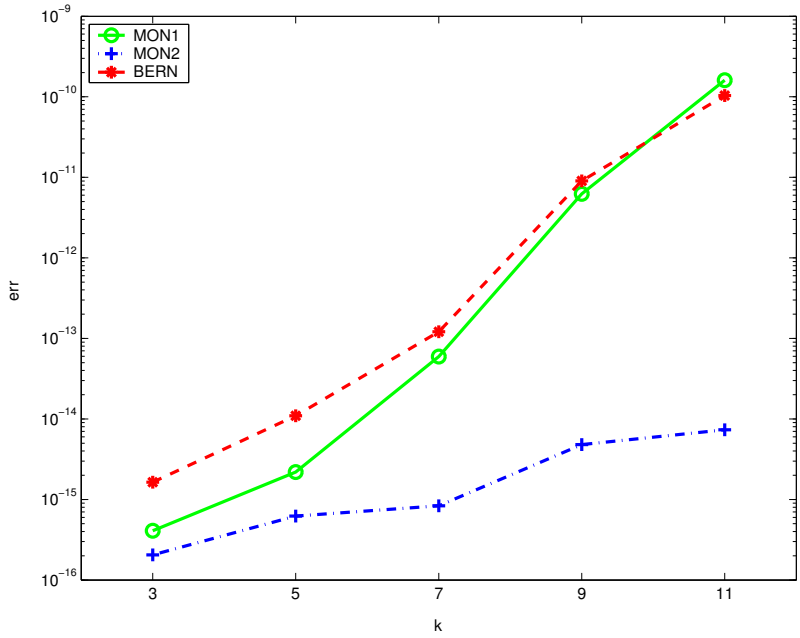

Figure 4: The k–step ETR on the uniform mesh. The relative error bounded in (19) with a standard computation of the right–hand side.

6 Conclusions

Our experiments show that the use of different bases and nodes to establish the order conditions can remarkably influence the accuracy in computing the coefficients of LMMs. In particular, among the three considered possibilities, MON1, which uses the monomial basis and the nodes between 0 and 1, is the worst even if it is the most natural one. The approaches MON2, which uses the monomial basis but the nodes both negative and positive, and BERN, which uses the Bernstein basis, are almost equivalent when the right–hand side is exactly represented. However, for some classes of methods such as the ETRs the right–hand side associated to BERN comes from previous computation and it can be affected by errors. In this case MON2 is the best choice. We outline that such formulation is implemented in the code TOM [10].

Appendix

Proposition 2 *The right–hand side of (7) for $j = 2$ has the following form*

$$\left[\mathbf{t}^{(i,2)}\right]_r = \frac{(-1)^r}{r+1}, \qquad r = 0, 1, \ldots, k.$$

Proof : First we observe that the vector $\mathbf{v}^{(i)}$ can be written as

$$\mathbf{v}^{(i)} = \int_{x_{i-1}}^{x_i} \mathbf{w}(x)\, dx,$$

where $\mathbf{w}(x)$ is defined according to (5). From the definition of the matrix $P_2^{(i)}$ given in (4) and by taking into account (6) we have

$$\begin{aligned}\mathbf{t}^{(i,2)} &= h_i^{-1} P_2^{(i)} \mathbf{v}^{(i)} = h_i^{-1} \left(D(h_i)\right)^{-1} \int_{x_{i-1}}^{x_i} P(-x_i)\, \mathbf{w}(x)\, dx = h_i^{-1} \left(D(h_i)\right)^{-1} \int_{x_{i-1}}^{x_i} \mathbf{w}(x - x_i)\, dx \\ &= h_i^{-1} \int_{x_{i-1}}^{x_i} \mathbf{w}\left(\frac{x - x_i}{h_i}\right) dx = \int_{-1}^{0} \mathbf{w}\left(t\right)\, dt.\end{aligned}$$

The thesis immediately follows. ∎

References

[1] L. Aceto and A. Sestini, On the numerical computation of the LMM's coefficients, (Editors: E. Simos, G. Psihoyios and C. Tsitouras), *Numerical Analysis and Applied Mathematics, AIP* 596-599(2007).

[2] L. Aceto and D. Trigiante, The matrices of Pascal and other greats. *Amer. Math. Monthly*, **108** no. 3, 232-245(2001).

[3] B.A. Björk and V. Pereyra, Solution of Vandermonde systems of equations. *Math. Comp.*, **24** no. 112, 893-903(1970).

[4] L. Brugnano and D. Trigiante, *Solving differential problems by multistep initial and boundary value methods*. Gordon and Breach Science Publishers, Amsterdam, 1998.

[5] C. de Boor, *A practical guide to splines*, Revised Edition Springer-Verlag, New York, Berlin, Heidelberg, 2001.

[6] G. Farin, Curves and surfaces for computer aided geometric design, Third Edition, Academic Press, Inc., San Diego, 1993.

[7] R.T. Farouki and T.N.T. Goodman, On the optimal stability of the Bernstein basis, *Math. Comp.*, **65** no. 216, 1553-1566(1996).

[8] N. J. Higham, Error analysis of the Björk–Pereyra algorithms for solving Vandermonde systems, *Numer. Math.*, **50** 613-632(1987).

[9] N. J. Higham, Stability analysis of algorithms for solving confluent Vandermonde–like systems, *SIAM J. Matrix Anal. Appl.*, **11** No. 1, 23-41(1990).

[10] F. Mazzia, *TOM code.* Available online at: `http://pitagora.dm.uniba.it/~mazzia/bvp/index.html`

[11] F. Mazzia, A. Sestini and D. Trigiante, B-spline linear multistep methods and their continuous extensions, *Siam J. of Numerical Analysis*, **44** No. 5, 1954-1973(2006).

[12] F. Mazzia, A. Sestini and D. Trigiante, BS linear multistep methods on non–uniform meshes, *JNAIAM*, **1** 131-144(2006).

[13] F. Mazzia, A. Sestini and D. Trigiante, The continuous extension of the BS linear multistep methods on non–uniform meshes, in press on APNUM.